Aerospace Science and Technology 56 (2016) 22–28

Contents lists available at ScienceDirect

Aerospace Science and Technology

www.elsevier.com/locate/aescte

Determination of stratospheric component behaviour using Finite Element model updating

J. Peeters [a,*], J. Van Houtte [d], A. Martinez [d], J. van Muiden [d], J.J.J. Dirckx [c], G. Steenackers [a,b]

[a] University of Antwerp, Op3Mech, Groenenborgerlaan 171, B-2020 Antwerp, Belgium
[b] Vrije Universiteit Brussel, Acoustics & Vibration Research Group, Pleinlaan 2, B-1050, Brussels, Belgium
[c] University of Antwerp, Biomedical Physics Lab, Groenenborgerlaan 171, B-2020 Antwerp, Belgium
[d] University of Antwerp, Elementary Particle Physics research group, Groenenborgerlaan 171, B-2020 Antwerp, Belgium

ARTICLE INFO

Article history:
Received 21 March 2016
Received in revised form 17 June 2016
Accepted 30 June 2016
Available online 7 July 2016

Keywords:
Finite element model updating
Thermal analysis
Inverse problem
Material characterization
REXUS/BEXUS

ABSTRACT

In general, it is difficult to analyse equipment for space applicability due to the fact that realistic tests on Earth are technically difficult and expensive. To prove the reliability of space systems, a combination of numerical analysis and expensive pre-flight tests is used. However, this paper discusses a new methodology in which a combination is made of low-budget ground tests with a newly developed finite element model updating technique which can deliver a time efficient added value or alternative to the expensive and time-consuming pre-flight tests during thermal analysis. In addition, this contribution shows the influence of several design parameters on the accuracy of thermal simulations for space applications and discusses how this accuracy can be optimised. The methodology is verified within the HACORD project of the REXUS/BEXUS programme.

1. Introduction

Scientific ballooning has been developed in the early 19th century, a few years after the invention of the hot air balloon by the Montgolfier brothers. This technique has been used frequently for scientific measurements since the entrance of low-density polyethylene balloons in the 1930s [1]. Even today, high altitude balloons are widely used in several disciplines e.g. atmospheric sciences, aeronautics, Earth observatory and physics on Earth and other planets [2]. The thermal design of spacecraft or balloon experiments is vitally important due to the extreme environmental conditions and zero-failure tolerances [3–5]. In general, thermal designs of balloon experiments are based on a combination of knowledge gained through previous experiments, empirical data and numerical simulations. Occasionally extra information is found by interpolating the environment at high altitude [6,3,5]. The use of accurate numerical models is essential to perform accurate simulations and to be able to design insulation techniques [7,8].

Finite element (FE) models, as explained in section 2.3, are widely used for virtual modelling and the prediction of the dynamic and the thermal behaviour of materials and lightweight structures [9,10]. These predictions are essential in the preparation of atmospheric balloon experiments [11,4,12]. Since atmospheric and space experiments are generally very expensive, it is important to have an excellent knowledge of the interaction between the experiment and its environment in advance, which is efficiently gained through reliable simulations. In general until now, these simulations are made only in steady state conditions and are mapped to a structural analysis [7,10]. Recent research compares these models manually with complex ground experiments which simulate the space environment as for example the NIRVANA facility, but these experiments are expensive to perform [10]. Next to its importance for predicting the response of the system, simulations are also crucial to increase confidence in advanced experiment set-ups operating in extreme conditions present in the upper atmosphere [8]. All material parameters and thermal loads of the experiment should be known in order to generate accurate estimations of the thermal behaviour [3].

Recent research, as performed by Liu et al. [13] tries to further improve these numerical models by using transient, time-dependent simulations in which the temperature and time-related parameters during the flight are approximated more accurately. The next step to improve the accuracy of the numerical models and predict the behaviour of balloon experiments is the combination of the numerical models with experimental measurements using numerical updating techniques like finite element model updating, known of system dynamics [14] and recently adapted to use for thermal models by Peeters et al. [15].

* Corresponding author.
E-mail address: jeroen.peeters2@uantwerpen.be (J. Peeters).
URL: http://www.op3mech.be (J. Peeters).

http://dx.doi.org/10.1016/j.ast.2016.06.024
1270-9638/

Nomenclature

c_p	Specific heat constant pressure	Pr	Prandtl number (dimensionless)
g_c	Gravitational acceleration	Ra	Rayleigh number (dimensionless)
Gr	Grashof number (dimensionless)	ΔT	Temperature difference from surface to air
h	Heat transfer coefficient	B	Coefficient of thermal expansion for air
k	Thermal conductivity of air	ρ	Density of air
L	Height or length of plate	μ	Dynamic viscosity of air
Nu	Nusselt number (dimensionless)		

For example, one of the important parameters in thermal radiation simulations which is essential to estimate correctly is the emissivity. This parameter is difficult to approximate correctly due to the influence of complex geometrical shapes [16].

The combination of an FE model of the structure with experimental data has major benefits because the experimental criteria can be relaxed due to the integration of the numerical model. Simple and fast to perform ground tests deliver enormous potential for FE updating, as part of a structural condition assessment program to use for correct approximate behaviour at extreme conditions.

The objective of this contribution is to predict the thermal insulation and heat distribution in the HACORD (High Altitude Cosmic Ray Detector) balloon experiment while being exposed to stratospheric conditions using two ground tests which are easy to perform: an actual long duration stratospheric flight and numerical simulations. The flight is made within the REXUS/BEXUS[1] programme using a balloon with a floating time of more than two hours at an altitude of 28.2 km.

To ensure accurate numerical simulations the finite element updating technique introduced in [15] is used for non-destructive evaluation. The technique is adapted for more general 3 dimensional thermal problems. The prediction results are validated using the real experimental data retrieved by thermal sensors during flight. The goal of this contribution is to validate if it is possible to better predict experimental device behaviour in space by using a straightforward thermal load and freezer experiment, performed in atmospheric conditions as input for an FE model updating routine. The described methodology can be used to accelerate the design process of atmospheric balloon experiments [5] and helps to improve the design process of future spacecraft [3].

2. Materials & methods

In the following section, we will describe the measurement techniques, the developed numerical model and the designed updating algorithm. The chapter starts with a brief description of the experimental box itself, after which the model and experiments will be discussed.

2.1. Experimental device description

The HACORD experiment consists of four Geiger–Muller tubes for the detection of cosmic ray particles and a PCB with an ARM® mBed™ micro-controller, a digital and analogue thermal sensor, three pressure sensors and the necessary power and communication electronics. The full system is packed in a polycarbonate box containing 8–20 mm of Styrofoam insulation and a reflective space blanket on the inside of the box to encapsulate the thermal heat of the PCB. The experimental components are shown in Fig. 1. A wireframe view of the full experiment is shown in Fig. 2 with the PCB (green), the Geiger–Muller tubes (red), the clamps (red), the Ethernet connector (red) and the power connector (yellow).

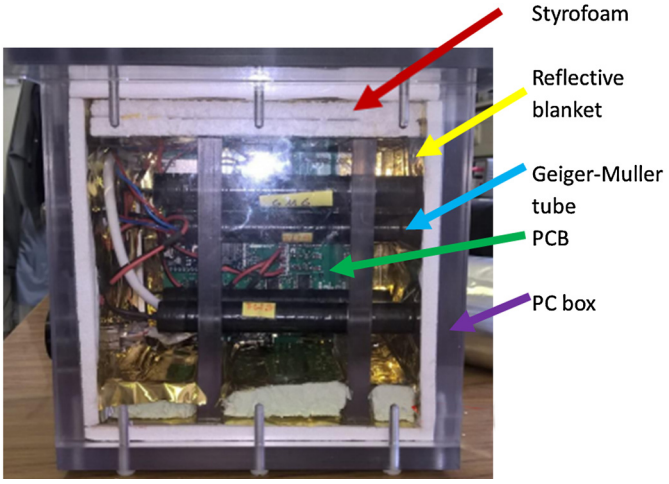

Fig. 1. Side view inside the experiment with in white the Styrofoam and in gold the reflective blanket.

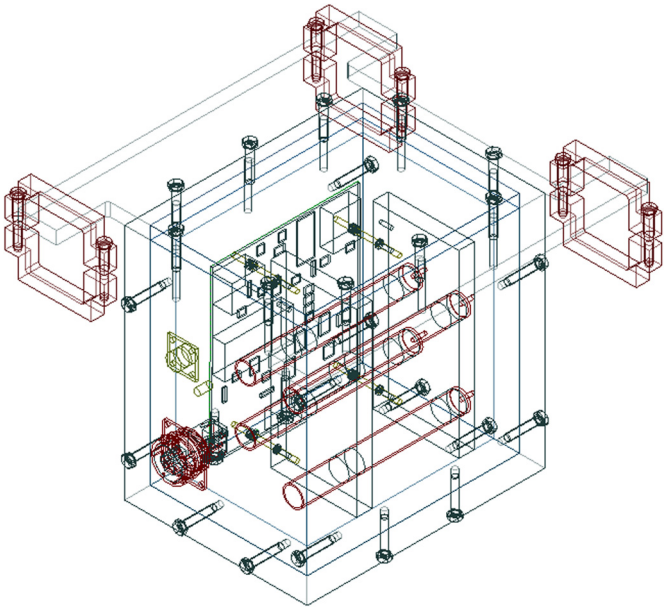

Fig. 2. Wireframe visual of the experiment design. (For interpretation of the references to colour in this figure, the reader is referred to the web version of this article.)

2.2. Description measurements

Three different types of measurements are performed: thermal load tests using a thermal imaging camera, a freezer test of the experimental box and finally the balloon flight.

[1] More information about the REXUS/BEXUS (Rocket/Balloon Experiments for University Students) programme can be found on www.rexusbexus.net.

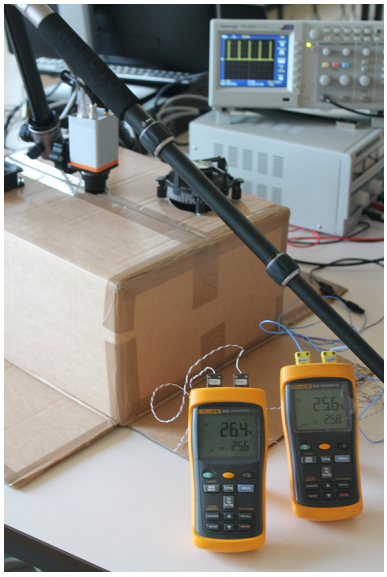

Fig. 3. Overview of the used experimental setup for the thermal load test.

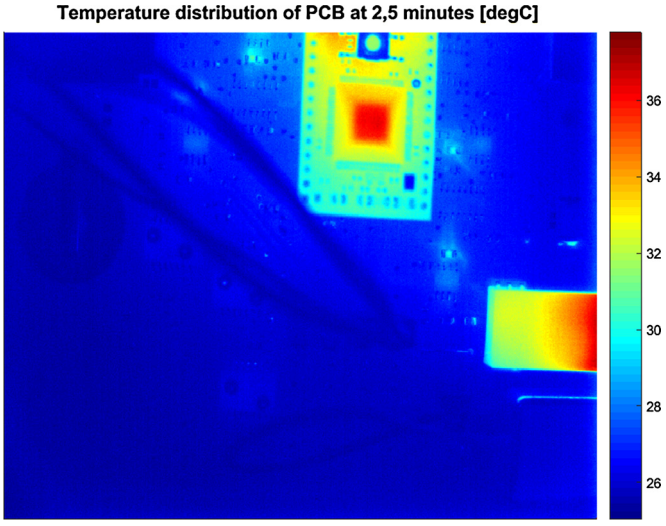

Fig. 4. Thermal image of the PCB during the thermal load test after 2.5 minutes.

2.2.1. Thermography of electronics

The thermal load monitoring test is performed using a thermal camera (Xenics Gobi 640Gige). The temperature increase of the PCB is monitored in a stabilised environment at an ambient temperature of 25.5 °C and atmospheric pressure starting from steady state disconnected to steady state under power. The temperature profile is measured during 30 minutes. After five minutes the temperature profile is stabilised to a steady state temperature. A photograph of the measurement set-up is shown in Fig. 3.

The temperature distribution of the PCB over time is used after post-processing [17,18] with the updating routine of section 2.4. To calculate the thermal loads of all the PCB components, the finite element updating techniques described in [15] is used. A frame of the PCB is shown in Fig. 4. An emissivity map is used to perform accurate thermal measurements and to extract the true temperature for each component during the heating phase.

2.2.2. Freezer test

Within this test, the thermal insulation capacity is measured from the retrieved thermal loads of the thermography test of section 2.2.1. The data of the two temperature sensors on the PCB were used: one NTC resistor below the ARM® mBed™ microcontroller and one digital sensor close to the DC/DC converters which are used to convert the supply voltage from the gondola to the needed high and low voltage for the PCB. Furthermore, four thermocouples have been placed in the experimental box:

- one on the High Voltage DC/DC converter;
- one in the centre of the box;
- one on the side wall above the reflective blanket;
- one below the reflective blanket, which is used to keep the heat radiation inside the box, on the same side wall.

For the test, the following procedure was followed. First, the experiment is switched on for 30 minutes inside the experimental box at room temperature to preheat the full system as in pre-flight conditions. Next, the box is placed in a freezer at a stable temperature of −80 °C for more than two hours, which is a simulation of the floating time in the balloon experiment. In this test the thermal isolation of the box could be tested for worst case scenarios where convection and radiation dissipation are considered.

2.2.3. Experimental flight BEXUS 20

The BEXUS 20 balloon with on board the HACORD experiment is launched from the balloon launch area of the Esrange space centre from SSC above the Arctic circle in Sweden. The BEXUS 20 atmospheric balloon reached an altitude of 28.2 km where it remained for 2 h and 10 min floating. During this flight, the temperature is measured at different locations on the PCB and in the experimental box:

- an NTC thermal resistor below the mBed™ controller on the PCB;
- a digital temperature sensor close to the DC/DC converters;
- a thermocouple type T on the outside wall of the polycarbonate box, shielded from cold air, wind and sunshine which measures the true temperature of the polycarbonate box;
- a thermocouple type T outside the gondola which measures the outside temperature.

The thermal and pressure data are logged at a rate of 1 measurement per second for the data from the PCB and 10 measurements per second for the external thermocouples. A representation of the temperature data is shown in Fig. 5.

2.3. Description numerical models

There is made use of the finite element method (FEM) to perform the numerical simulations, which is a computational technique used to approximate complex boundary value problems by subdividing the large structure in a mesh of connected calculation elements. These mesh elements have dependent variables which must satisfy the standard heat equation and specific boundary conditions within the known domain of the experiment, described by the independent environment variables. This problem will be approximated by iteratively solving the describing differential equations with its boundary values for each element on each time step until the problem converges [19,7].

Finite element model The numerical simulations are performed in the commercial Siemens NX 10 finite element software which solves the FEM using the NX Thermal solver, which is based on the I-deas™ TMG solution which uses a conservative, element-based control volume formulation [20]. There is made use of specifically adapted meshes with in total 154 774 non-linear tetrahedral elements and 235 438 nodes with thermally dependent material properties as shown in Fig. 6. The calculation time for the full

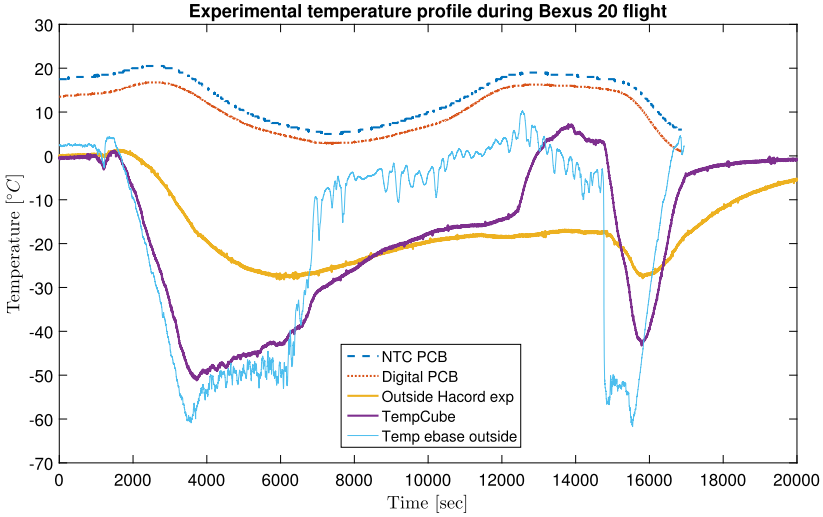

Fig. 5. Experimentally measured temperatures for all thermocouples during BEXUS 20 flight.

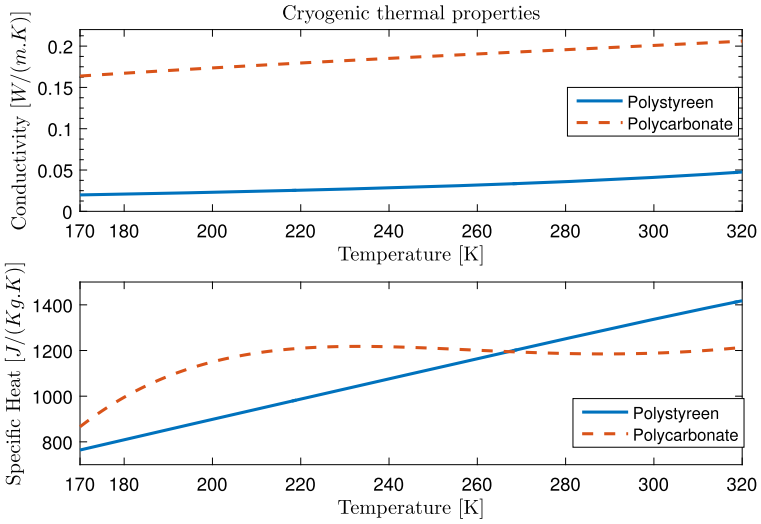

Fig. 6. Temperature dependent material properties of the polycarbonate box and the Styrofoam insulation.

model was approximately 330 minutes on a desktop PC with 32 GB ram and a 3.2 GHz octa-core CPU approximately 330 minutes.

A representation of the meshed internal structures with the loading on the PCB is shown in Fig. 7.

Physics & boundary conditions The ambient pressure and temperature are related to the local ambient temperature according to the flight profile. The results of the numerical model, with the thermal profile measured outside, are used to compare the standard data and the updated simulation data. As shown in the simplified formula of Eq. (1) to Eq. (3), the convective heat transfer varies quadratic with the air pressure or density as shown in Eq. (3) derived in [21].

$$Nu = C(Gr.Pr)^n = CRa^n \tag{1}$$

$$h = \frac{k}{L}.C(\frac{\rho^2 g_c \beta c_p \Delta T L^3}{\mu^2}.\frac{\mu}{c_p k}) \tag{2}$$

or

$$h \sim \rho^2 \tag{3}$$

The thermal loads are updated using information from the thermal load test of the PCB. Hemicubes and view factors are used to calculate radiation by dividing each mesh element into three parts in such a way that the thermal coupling between the different components inside the box and the radiation to the outside of the polycarbonate box. The reflective blanket is implemented in the thermo-optical parameters of the mesh. The literature on this subject shows that the IR reflectance of these thermal space blankets equals 0.95 and the emissivity/absorbance of solar radiation is 0.05 [22].

From the experimental data shown in Fig. 5, one can see that the solar radiation causes a significant temperature drift during the float stage which influences the temperature profile of the electronic components. This can be deduced from the temperature rise between 6000 and 14000 seconds where the balloon remains floating at its maximum altitude. In contrast to what is expected, the measured temperature rises, first starting in the outside thermocouples. This proves that the influence is coming from outside the box. The irradiation due to the current solar flux can be predicted using the geometrical coordinates, altitude, date and time considering the inclination of the sun for an eastbound balloon flight. Besides an Albedo factor[2] of 0.15 is considered typical for the for-

[2] Reflection factor due to the Earth surface. It represents the fraction of solar energy reflected from the Earth back into space [23].

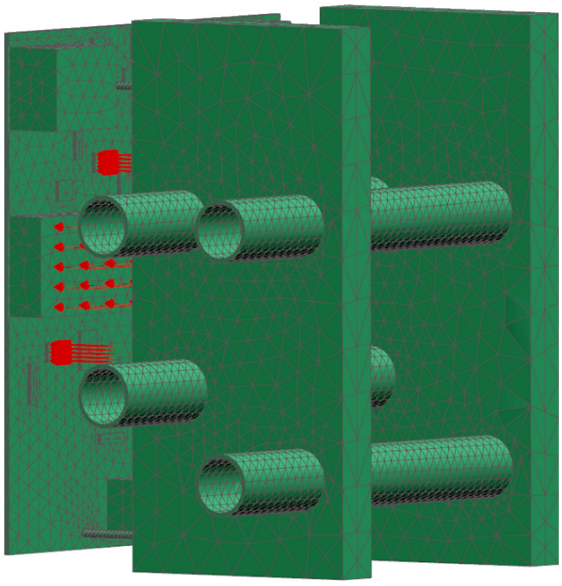

Fig. 7. Simulated internal structure with tetrahedral mesh.

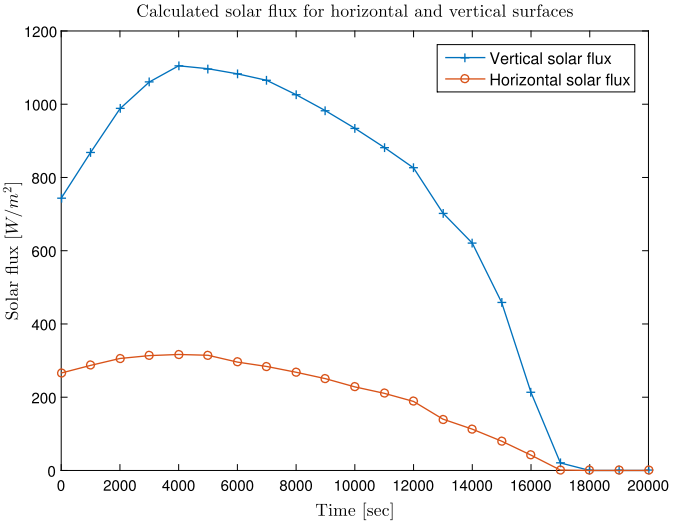

Fig. 8. Evolution of the solar fluxes during the flight in the East direction.

est vegetation of Lapland and a clear sky factor of 1 is chosen as visual contact remains over approximately 100 km. The solar flux is calculated for each time step considering the solar time and the altitude of the gondola. A plot of the time variance of the solar flux is shown in Fig. 8.

2.4. Updating algorithm

The updating algorithm works in two different stages where the targets are set to update the numerical model of the BEXUS 20 flight simulation:

1. The experimental data of the thermal load test is used as a target to estimate the thermal loads on the PCB.
2. The experimental data of the freezer test are used as a target to estimate the insulation properties of the full assembly.

The optimisation uses the relative temperature differences $\vartheta = T_{numerical} - T_{target}$ as objective function to accurately estimate the thermal behaviour in a near-space environment. The algorithm has no fixed amount of iterations, in contrast to the method described in [24], and is based on the methodology described in [15]. The parameter *stability control* is increased even for the use of dependent parameter sets and the use of multiple initial values for each parameter set, in contrast to the method described in [15]. In a first stage, a meta-model is created of a response surface built out of $2*n-2$ data points for $n > 2$. This surface is retrieved from numerical simulations that are randomly distributed across the design space. The design space is built out of the physical boundary values for each parameter of the objective function. This meta-model is built out of n-dimensional polynomials, each dimension representing an unknown parameter and forming one single n-dimensional response surface together with all the other dimensions. The optimisation algorithm searches for a global minimum of the objective function in the meta-model which results in estimated values for each parameter. The estimated parameter values are the input of a new numerical model, called the updated numerical model. The results of this updated numerical solution have a higher correlation with the experimental target values and deliver new input that could replace the least accurate data point inside the meta-model with the more accurate data point of the last solution. This iterative process reforms the response surface locally in the region of the global minimum. The local conversion of the response surface is a local solution of the optimisation problem. The simultaneous use of different values delivers a conversion to a global minimum. This process continues until convergence is achieved for the error value between the experimental values and the minimum of the meta-model. The optimiser is a least square curve fitting optimiser following the trust region regression algorithm conform to [15]. In [15] this is explained as the most efficient.

3. Results & discussion

In the following section, the results of the two different updating routines will be discussed and the influence of the updating on the numerical simulation will be shown. Finally, both the updated and the normal numerical model will be compared with the retrieved experimental data of the BEXUS 20 flight.

3.1. Comparison thermal load PCB

In a first stage, a comparison was made between the numerical model of the thermal load test and the experimental thermography data. As the composition of the PCB is well known and the ambient conditions are controlled as explained in section 2.2.1, the only difference between the numerical model and the experimental data are the effective thermal loads of the components and the heat distribution over the PCB. Using the updating routine of section 2.4, the thermal load values in Table 1 are retrieved. It is clearly shown that the overall thermal load is a little bit higher than the assumed thermal loads derived from data sheets: 1.68 W instead of 1.4 W which is verified by the true power consumption of 0.06 A at 28 V of the PCB. To perform the updating process, the temperature response is compared for the different components during the start of the experiment until steady state conditions are achieved.

From these results, we can conclude that the overall power consumption can be predicted from data sheet information in combination with a global power test. However, if the power distribution over the PCB is important to balance the heat distribution or adapt the thermal insulation to the local power consumption, an accurate simulation with accurate values is necessary. Table 1 shows that after updating the thermal loads the distribution over the PCB is more precise and the summation is accurately close to the global power consumption.

Table 1
Comparison thermal loads on PCB assumed from datasheets and after updating from the thermal load test.

Component	Assumed [W]	Updated [W]
High Voltage DC/DC Converter	0.3	0.17
Voltage Comparator	0.2	0.07
DC/DC Step Down Converter	0.3	0.42
mBed microcontroller	<0.1	0.84
Remaining components	< 0.01 (total ≈ 0.1)	total ≈ 0.18
Summation global Power consumption	1.4	1.68

3.2. Comparison isolation parameters

In a second stage, after the thermal loads on the PCB are updated correctly, the heat transfer parameters must be made more accurate. The most important parameters are the heat transfer coefficients of the experimental box, the conductivity of the PCB, the specific heat of the PCB and the emissivity of the box. The emissivity map of the PCB is already known from the thermal load test of section 2.2.1, discussed in the previous section and the conductivity and specific heat of the Styrofoam and polycarbonate are calculated analytically as a function of the temperature as described in section 2.3. To update the numerical model of the freezer test, the temperature sensors were used as described in section 2.2.2 as target data and the updating routine of section 2.4. A comparison of the experimental temperature profile and the updated profile is shown in Fig. 9 for the thermocouple of the high voltage DC/DC converter and ambient temperature in the centre of the box.

As could be seen in Fig. 9, the thermal behaviour of the numerical model of the freezer test corresponds with the experimental data. The largest error is seen when the box is placed from the ambient climate into the freezer. This little time instance, however, has a limited effect on the characterisation of the isolation parameters.

3.3. Prediction thermal flight data using updated model

After the updating of the thermal load parameters in section 3.1 and the material parameters in section 3.2, the same numerical model is used to simulate the balloon flight with the decrease of convection depending on the altitude and the insolation as described in section 2.3. In the results, shown in Fig. 10, a comparison has been made between the experimental data, the numerical model before and after updating the parameters. The temperature profile of the different measurement spots, including the imposed ambient temperature is shown as discussed in section 2.2.3.

Fig. 10 shows that the thermal parameters have a major influence on the temperature evolution of the PCB components. Without updating the numerical model, a major drift in the heat dissipation caused by insolation during float can be detected by looking at the two sensors inside the box. After updating the thermal loads and thermal properties the numerical model predicts the experimental measurements with an improved accuracy. The root-mean-square error for the difference between the numerical and experimental data improves by a factor 2.2 to 7.6 for each time interval due to the updating. The major discrepancy is seen around 16000 seconds. At this time step, the balloon is cut and the gondola encounters a brief free fall back to earth before the parachute opens. It is assumed that the fast movement of the gondola and the fast temperature and pressure gradients cause the divergence as this dynamic movement of the gondola is not considered in the simulation model.

4. Conclusions

A numerical model, used to predict the thermal behaviour of stratospheric balloon experiments, can be updated through a limited number of ground tests. When the environmental conditions are well described, but contain a number of uncertain parameter values, the updating routine delivers a major accuracy improvement by a factor of 2.2 to 7.6. This method can also be used for other well-known complex environment estimations as a replacement for expensive, long duration and/or dangerous experiments. The boundary conditions of the method are that the uncertain parameter values are independent of the experiment environment. Moreover, the methodology can be used to validate experimental designs for space applications and determine the failure risk of different components or design versions in a fast and cost-efficient way.

Conflict of interest statement

Conflicts of interest: none.

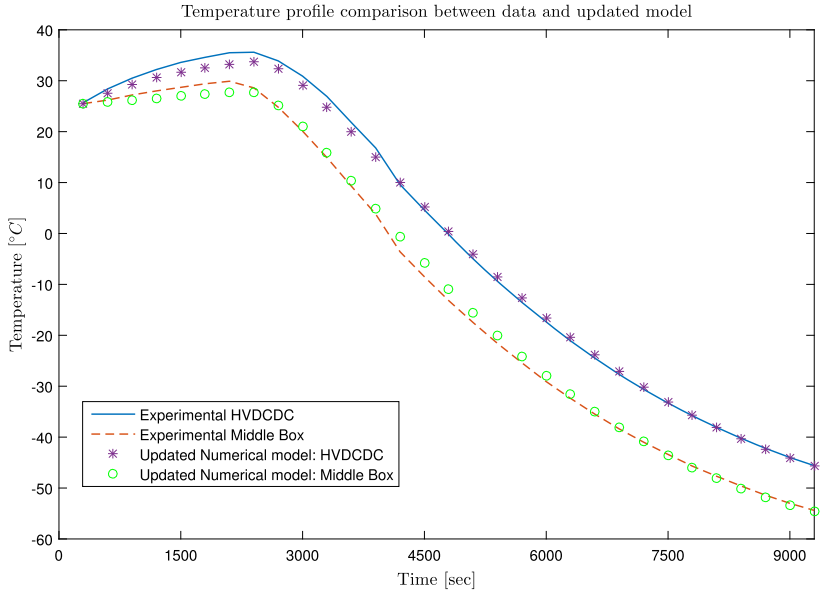

Fig. 9. Comparison of the temperature evolution of the numerical model and the experimentally measured data from the thermocouples.

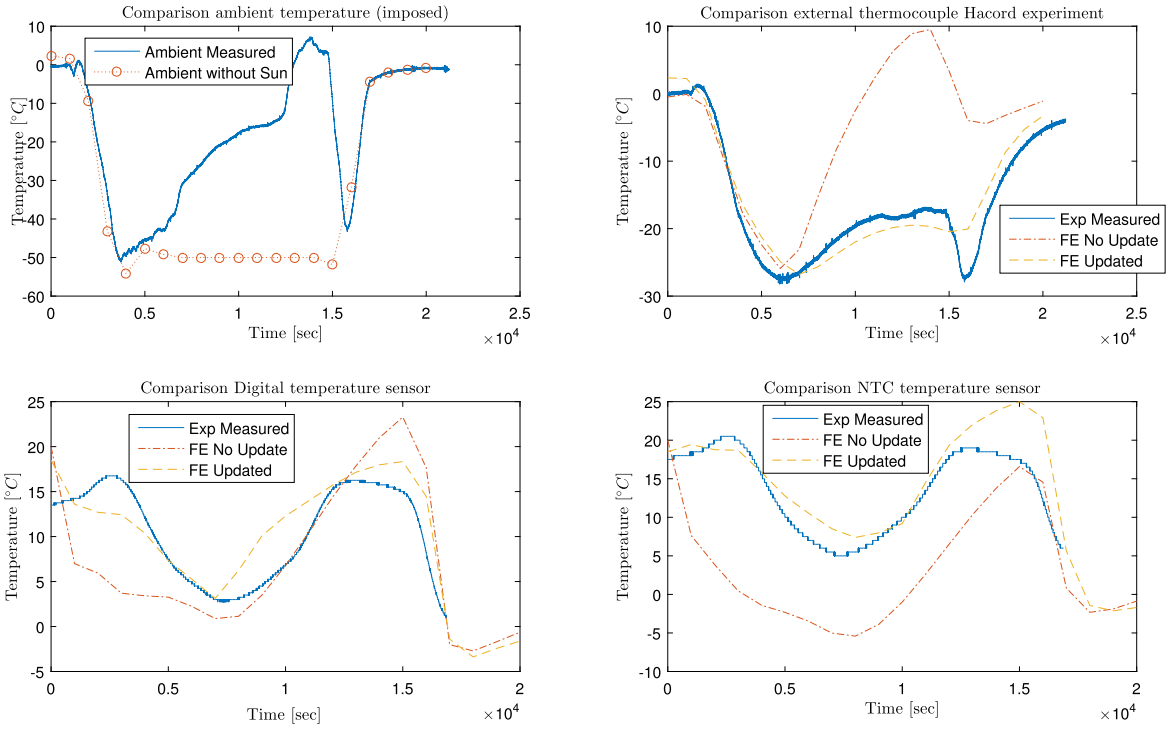

Fig. 10. Comparison between the temperature evolutions of the numerical model and the experimentally measured data from the flight data.

Acknowledgements

This research has been funded by the University of Antwerp (Belgium) and the Institute for the Promotion of Innovation by Science and Technology in Flanders (IWT) by the support to the TETRA project 'Smart data clouds' with IWT project number 140336. Furthermore, the research leading to these results has received funding from Industrial Research Fund FWO Krediet aan navorsers 1.5.240.13N and the FWO travel grant V4.010.16N. The authors also acknowledge the REXUS/BEXUS programme and their sponsors ESA, DLR, ZARM, SSC and SNSB for their support and the organisation of the BEXUS 20 flight of the HACORD experiment.

Appendix A. Supplementary material

Supplementary material related to this article can be found online at http://dx.doi.org/10.1016/j.ast.2016.06.024.

References

[1] M. Gai, G. Guglieri, M.G. Lattanzi, A. Lombardi, M. Mana, L. Masserano, I. Musso, P. Navone, A scientific mission based on a high altitude stratospheric balloon, Int. J. Aerosp. Sci. 3 (1) (2014) 18–29, http://dx.doi.org/10.5923/j.aerospace.20140301.03.

[2] J.L. Stecher, in: 20th Space Simulation Conference, The Changing Testing Paradigm, October 27–29, NASA, NASA/CR, 1998, p. 319.

[3] D. Swanson, Spacecraft thermal control systems, Tech. rep., NASA, 2001.

[4] A. Vargas, C. Tarrieu, J.-P. Lepage, P. Mauroy, C. Sirmain, Mars balloon simulator, Acta Astronaut. 26 (8) (1992) 697–706.

[5] Y. Nobuyuki, I. Naoki, I. Takeshi, A. Toyoo, Scientific Ballooning: Technology and Applications of Exploration Balloons Floating in the Stratosphere and the Atmospheres of Other Planets, Springer, 2009.

[6] F. Kreith, Thermal design of high-altitude balloons and instrument packages, J. Heat Transf. 92 (3) (1970) 307–332.

[7] S. Wachche, A. Marne, S. Singare, P. Naik, O. Bhide, G. Chaudhari, P. Vartak, S. Pendse, C. Tadwalkar, Thermal modeling and simulation of a Pico-satellite using Finite Element Method, in: L. Ferguson, R. Goldstein, S. MacKenzie, R. Papp (Eds.), 5th International Conference on Thermal Process Modeling and Computer Simulations, ASM International, Orlando, 2014, pp. 65–74.

[8] S. Lapensée, C. Alary, Development and analysis of the surface thermal environment for the ExoMars lander mission, in: 40th International Conference on Environmental Systems, ICES 2010, 2010, pp. 1–22.

[9] A. Abdul-Aziz, Assessment of crack growth in a space shuttle main engine first-stage high-pressure fuel turbopump blade, Finite Elem. Anal. Des. 39 (2002) 1–15, http://dx.doi.org/10.1016/S0168-874X(02)00058-6.

[10] P. Vialettes, J.M. Siguier, P. Guigue, M. Karama, S. Mistou, O. Dalverny, S. Granier, F. Petitjean, Experimental and numerical simulation of super-pressure balloon apex section: mechanical behavior in realistic flight conditions, Adv. Space Res. 37 (11) (2006) 2082–2086, http://dx.doi.org/10.1016/j.asr.2005.04.064.

[11] E.S. Seo, H.S. Ahn, S. Beach, J.J. Beatty, S. Coutu, M.A. DuVernois, O. Ganel, Y.J. Han, H.J. Kim, S.K. Kim, M.H. Lee, L. Lutz, S. Nutter, S. Swordy, J.Z. Wang, Cosmic-Ray energetics and mass (CREAM) balloon experiment, Adv. Space Res. 30 (5) (2002) 1263–1272, http://dx.doi.org/10.1016/j.asr.2003.05.019.

[12] D. Balagangadhar, S. Roy, Design sensitivity analysis and optimization of steady fluid-thermal systems, Comput. Methods Appl. Mech. Eng. 190 (2001).

[13] Q. Liu, Z. Wu, M. Zhu, W.Q. Xu, A comprehensive numerical model investigating the thermal-dynamic performance of scientific balloon, Adv. Space Res. 53 (2) (2014) 325–338, http://dx.doi.org/10.1016/j.asr.2013.11.011.

[14] T. Marwala, Finite-Element-Model Updating Using Computational Intelligence Techniques, Springer, 2010.

[15] J. Peeters, G. Arroud, B. Ribbens, J. Dirckx, G. Steenackers, Updating a finite element model to the real experimental setup by thermographic measurements and adaptive regression optimization, Mech. Syst. Signal Process. 64–65 (2015) 428–440, http://dx.doi.org/10.1016/j.ymssp.2015.04.010.

[16] J. Peeters, B. Ribbens, J.J.J. Dirckx, G. Steenackers, Determining directional emissivity: numerical estimation and experimental validation by using infrared thermography, Infrared Phys. Tech. 77 (2016) 344–350, http://dx.doi.org/10.1016/j.infrared.2016.06.016.

[17] X. Maldague, Theory and Practice of Infrared Thermography for Nondestructive Testing, Wiley, Quebec, 2001.

[18] M. Vollmer, K. Möllmann, Infrared Thermal Imaging: Fundamentals, Research and Applications, Wiley-VCH, Berlin, 2010.

[19] O.C. Zienkiewicz, R. Taylor, The Finite Element Method, vol. 1–3, 5th edition, Butterworth Heinemann, Oxford, 2000.

[20] (Siemens), I-DEAS TMG Thermal Analysis, 2015.

[21] T.L. Bergman, A.S. Lavine, F.P. Incropera, D.P. DeWitt, Fundamentals of Heat and Mass Transfer, 7th edition, John Wiley & Sons, Incorporated, 2011.

[22] L. Viennot, N. Décamp, Which side to put the survival blanket? Analysis and suggestions for activities with students, Tech. rep. July, Physics Education Division (PED) of the European Physical Society (EPS), 2014.

[23] J.P. Holman, Heat Transfer, 6th edition, McGraw-Hill, 1990, arXiv:1011.1669v3.

[24] G. Steenackers, F. Presezniak, P. Guillaume, Development of an adaptive response surface method for optimization of computation-intensive models, Comput. Ind. Eng. 57 (3) (2009) 847–855, http://dx.doi.org/10.1016/j.cie.2009.02.016.